UKaaZ

Annals of Phytomedicine 6(2): 63-73, 2017
DOI: 10.21276/ap.2017.6.2.5; Print ISSN : 2278-9839 and Online ISSN : 2393-9885

Ann. Phytomed.,
6(2): 63-73 (2017)

Original article

Characterization of 1-deoxy-D-xylulose 5-phosphate synthase (DXS) protein in *Andrographis paniculata* (Burm.f.) Wall. ex. Nees: A *in silico* appraisal

Mote Srinath, Aayeti Shailaja, Byreddi Bhavani Venkata Bindu and Charu Chandra Giri
Centre for Plant Molecular Biology (CPMB), Osmania University, Hyderabad-500007, Telangana State, India.

Received October 18, 2017: Revised November 30, 2017: Accepted December 10, 2017: Published online December 30, 2017

Abstract

Andrographis paniculata (Burm.f.) Wall. ex Nees is as an important medicinal plant from centuries for treating infectious diseases in India and other countries. Active principles of this plant are diterpene lactones, specifically andrographolides and are synthesised *via* two independent biosynthetic pathways, *i.e.,* mevalonic acid (MVA) and methyl-erythritol phosphate (MEP) pathway. Very meagre genomic and proteomic information is available about the genes and enzymes involved in these biosynthetic pathways. In this study, we have performed *in silico* characterization of a vital rate limiting enzyme 1-deoxy-D-xylulose 5-phospahte synthase (DXS) of MEP pathway in *A. paniculata*. Structural and functional characterization of *A. paniculata* DXS *(Ap*DXS*)* revealed its hydrophobic nature and a non trans-membrane protein was found to be present in chloroplast stroma. Predicted 3D structure with phyre2 tool had shown 85% of amino acids in the most favoured region as revealed by Ramachandran plot and was 96.32% structurally reliable. The phylogenetic analysis of *Ap*DXS by MEGA7 revealed evolutionarily close relationship with Lamiaceae (*Phlomis umbrosa/ Phlomoides umbrosa, Plectranthus barbatus, Lavandula angustifolia* and *Salvia miltiorrhiza*) and Pedaliaceae (*Sesamum indicum*) families. Protein-protein interaction study revealed the interface of *Ap*DXS with other MEP pathway proteins such as HDS, HDR, DXR and CDPMEK. Further, interaction was also evident with MVA pathway protein HMGS and downstream proteins, *viz*., GPS1, IPPI1 of diterpenoid pathway. The findings on the interactions of *Ap*DXS with HMGS has given insight to the cross talk between MEP and MVA pathways. Prediction of bio-physico-chemical properties, secondary and tertiary structures will be of significance in protein purification processes. In addition, it will also be advantageous for drug designing applications with particular reference to manipulation of biosynthetic pathway, involving diterpene lactones in *A. paniculata*.

Keywords: *Andrographis paniculata* (Burm.f.). Wall. ex. Nees, *Ap*DXS protein, 3D structure, phylogenetic analysis, Ramachandran plot, protein-protein interactions

1. Introduction

Andrographis paniculata (Burm.f.). Wall. ex. Nees, a well-known medicinal plant used for treating various diseases in herbal medicaments and botanicals (Akbar *et al*., 2011; Subramanian *et al*., 2012; Hossain *et al*., 2014; Okhuarobo *et al*., 2014; Sharma *et al.*, 2017; Hu *et al*., 2017; Nyeem *et al*., 2017). The synthesis of diterpene lactones mainly andrographolides coordinated *via* two independent pathways mevalonic acid (MVA) and methyl erythritol phosphate (MEP) pathways, (Figure 1) in cytosol and plastids, respectively (Eisenreich *et al*., 2004; Srivatsava and Akhila, 2010). These two pathways are independent, however; a cross talk between them do exist (Rodríguez-Concepción *et al*., 2015; Mendoza-Poudereux *et al*., 2015). Glyceraldehyde-3-phosphate and pyruvate are starting molecules in MEP pathway and the first reaction is catalysed by 1-deoxy-D-xylulose 5-phosphate (DXP) synthase (DXS) enzyme (Rohmer *et al*., 1996; Lange *et al.*, 1998; Lois *et al*., 1998; Zhao *et al*., 2013; Frank *et al*., 2016). DXS is identified as the rate limiting key enzyme of MEP pathway (Harker and Bramley, 1999; Kuzuyama *et al*., 2000; Banerjee and Sharkey, 2014; Rodríguez-Concepción *et al*., 2015). Modification of DXS expression was found to alter the isoprenoids production in *Catharanthus roseus* (Chahed *et al*., 2000), *Ginkgo biloba* (Morris *et al*., 2006), potato (Morris *et al*., 2006), tomato (Enfissi *et al*., 2005; García *et al*., 2017), *Withania* (Jadaun *et al*., 2017) and *Arabidopsis* (Estevez *et al*., 2001; Wright *et al*., 2014). These findings substantiated the rate limiting characteristics of DXS in the MEP pathway. Structural and functional information of rate limiting enzymes of these pathways is paramount in the study of biochemical properties for isolation of the protein, elucidating the 3D protein models for drug designing and protein interaction studies

Author for correspondence: Dr. Charu Chandra Giri
Professor, Centre for Plant Molecular Biology (CPMB), Osmania University, Hyderabad-500007, Telangana State, India
E-mail: giriccin@yahoo.co.in
Tel.: +91-040-27098087

in the biosynthesis of secondary metabolites (Elizabeth *et al.*, 2011; Singh *et al*, 2014; Bindu *et al*, 2017). The modification of metabolic flux *via* altering the DXS expression increases the scope for increased synthesis of diterpene lactone ultimately elevated andrographolide production (Pulido *et al.*, 2012; Simpson *et al.*, 2016). In plants, DXS is encoded by a small gene family where three groups have been reported (Lange *et al.*, 1998; Walter *et al.*, 2002; Krushkal *et al.*, 2003; Rodriguez-Concepion *et al.*, 2004; Kim *et al.*, 2008; Phillips *et al.*, 2008; Cordoba *et al.*, 2009, 2011). Group III DXS family is involved in secondary metabolism and defense responses (Zhou *et al.*, 2016). In response to the IPP and DMAPP levels, DXS protein levels are post transcriptionally regulated (Guevara-García *et al.*, 2005; Henriquez *et al.*, 2016; Kudoh *et al.*, 2017).

Further, in our laboratory we have an inclusive research agenda involving studies on the distribution of *A. paniculata* and related species, haplotyping, selection and yield augmentation of bioactive compounds, using biotechnological and molecular approaches (Neeraja *et al.*, 2015; Arolla *et al.*, 2015; Parlapally *et al.*, 2015; Zaheer and Giri, 2015; Neeraja *et al.*, 2016; Bindu *et al.*, 2017; Zaheer and Giri, 2017a; Zaheer and Giri, 2017b). In the present communication, we report the *in silico* investigation on structural, functional and evolutionary inter relationships of *Ap*DXS and its interaction with MVA and MEP pathway proteins.

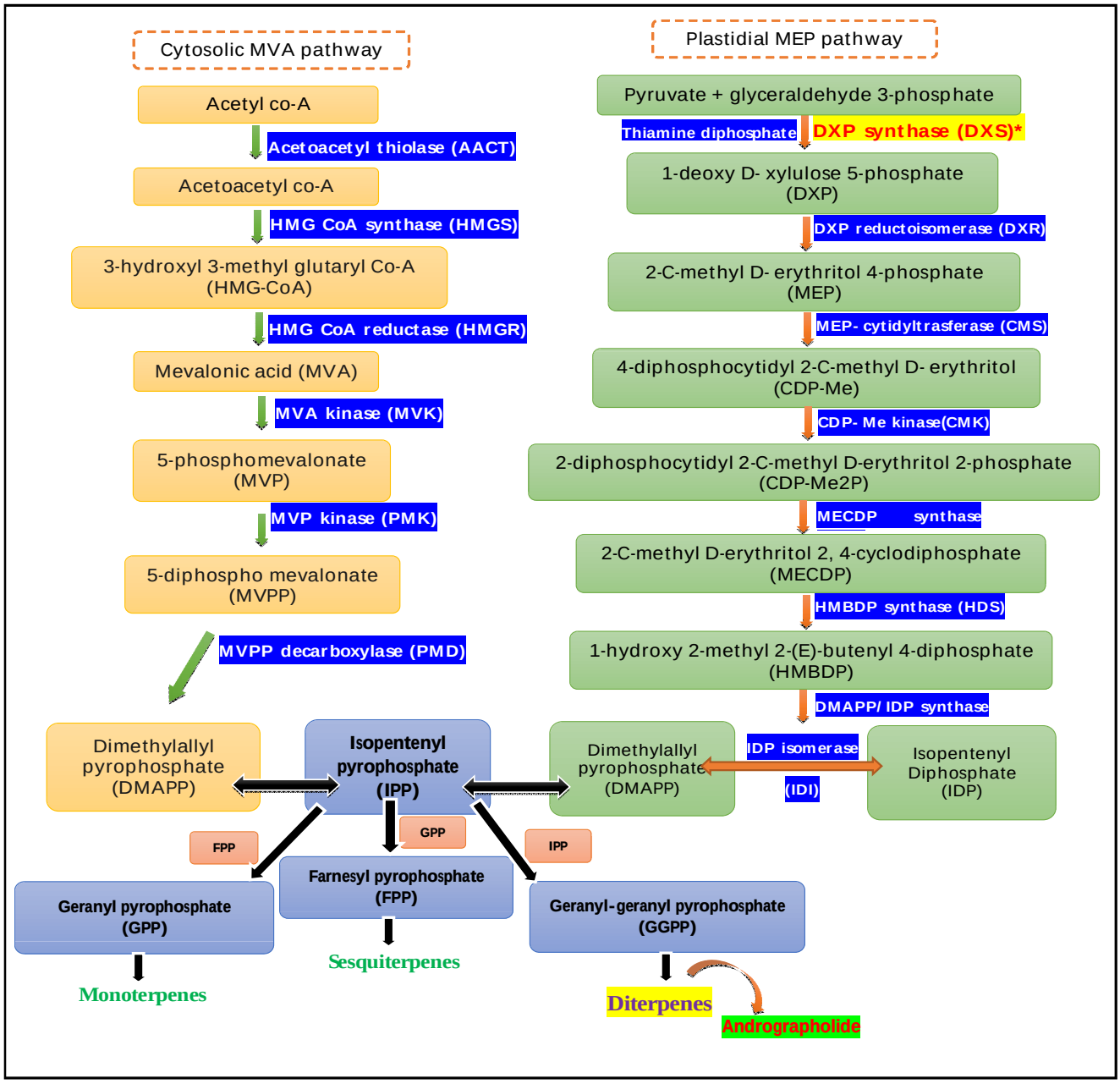

Figure 1: MVA/MEP pathways for diterpene lactone andrographolide biosynthesis.

2. Materials and Methods

2.1 Calculation of physico-chemical properties of *Ap*DXS

Protein sequence was collected from NCBI (Accession Number: AAP14353.1) in FASTA format which is of 691 amino acid long. Amino acid composition was anticipated by Predict protein open tool (Rost *et al*., 2004). Protein molecular weight and isoelectric point were calculated using ExPASy ProtParam (Colovos and Yeates, 1993), compute pI/MW (Bjellqvist *et al.*, 1993, 1994; Gasteiger *et al*., 2004) and JVirGel (Hiller *et al*., 2006) tools. Hydropathy plots were plotted using Kyte-Doolittle method (Kyte and Doolittle, 1982) and histograms of physico-chemical properties were analysed through EMBOSS PepInfo tool (Eisenberg *et al*., 1982; Kyte *et al*., 1982; Sweet *et al*., 1983).

2.2 Elucidation of secondary structure, sub-cellular location and signal peptide

PHD secondary structure prediction method was followed for the secondary structure elucidation of *Ap*DXS protein as per Roast and Sandor, 1983. ChloroP, MitoP, SignalP, TargetP (Emanuelsson *et al*., 2007), iPSORT (Bannai *et al*., 2001, 2002) and PrediSi (Hiller *et al*., 2004) were used to find out the sub cellular location and signal peptide sequence of *Ap*DXS.

2.3 Motifs and domain analysis in *Ap*DXS

The prediction of trans-membrane helices and presence of surface globular proteins was carried out using, trans-membrane topology prediction server, Hidden Markov Model Topology of Proteins (HMMTOP) as per Tusnady and Simon (2001). The Tied Mixture Hidden Markov Model (TMHMM), and "Dense Alignment Surface" (DAS) algorithm based trans-membrane (DAS-TM) filter servers were also used (Cserzo *et al.*, 1997). The presence of trans-membrane beta barrel was envisaged using Prediction of Trans-membrane Beta Barrel (PRED-TMBB) following the tool as reported by Bagos *et al*., 2004a, 2004b. Prediction of domains was carried out by Interpro and loop-length-dependent support vector machine (DLP-SVM) tool as per Ebina *et al.*, 2009 and Finn *et al.*, 2017. Motif analysis was carried out using Pfam tool (Finn *et al*., 2016).

2.4 3D structural modelling and its validation

3D structural model of *Ap*DXS was predicted using Phyre2 tool (Kelley *et al*., 2015) and validated with SAVES-PROCHECK (Laskowski *et al*., 1993). Ligand binding sites were predicted using 3DLigandSite tool (Wass *et al*., 2010). 3D model generated by Phyre2 in PDB format was used as template for finding the ligand clusters.

2.5 Evolutionary relationships of *Ap*DXS with other organisms

*Ap*DXS sequence was subjected to different blast analyses (blatsp, PSI blast and blast PDB) against non-redundant protein sequences, model organisms and uni-protKB/swiss-protein sequences (Altschul *et al*., 1997). Total 38 sequences were selected for phylogenetic tree construction including model plants like *Arabidopsis thaliana* and *Oryza sativa*, model organisms *Homo sapiens*, *Escherichia coli*, *Drosophila melanogaster* and *Mus musculus*. Plants showing more than 80% identity were selected (except *H. sapiens, E. coli, D. melanogaster* and *M. musculus*) and used for the construction of phylogenetic tree. All positions containing gaps and missing data were eliminated. Total of 568 positions were present in the final dataset. Molecular evolutionary genetics analysis (MEGA) was conducted by maximum likelihood method using MEGA7 software (Kumar *et al*., 2016).

2.6 Search tool for the retrieval of interacting genes/protein (STRING) analysis

Protein-protein interactions (PPI) was predicted by using STRING10 tool (Szklarczyk *et al*., 2014). *A. thaliana* was taken as template (as *Ap*DXS was showing 85% identity with query cover 95%). Parameters were changed to specifically identify interaction with MEP and MVA pathway related proteins. Coexpression analysis of *Ap*DXS with other interacting proteins was performed using *Arabidopsis* and other organisms as templates.

3. Results and Discussion

3.1 Elucidation of physico-chemical properties of *Ap*DXS

*Ap*DXS protein has a theoretical molecular weight (74489.81D) with an isoelectric point of 6.5. The amino acid composition in primary structure and percentages of amino acids are depicted in Figures 2, 3 and Table 1. From the hydropathy plots, it was found that *Ap*DXS was not having any trans-membrane region as no peaks were observed with scores greater than 1.8 as shown in the hydropathy plot of reading window 19 (Figure 8A). In the reading window 9, there were no strong peaks with negative score indicating that no presence of surface globular proteins (Figure 8B). Biochemical properties such as aromaticity, aliphatic nature, negatively and positively charged amino acids were also observed (Figure 9).

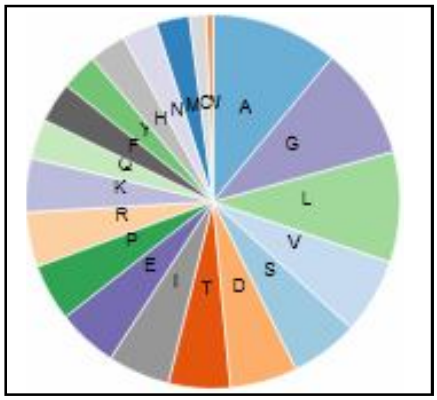

Thr(T)- ; Ile(I)- ; Glu(E)- ; Pro(P)- ; Arg(R)- ;Lys(K)- ;Gln(Q)- ;Phe(F)- ;Tyr(Y)- His(H)- ; Asp(N)- ; Met(M)- ;Cys(C)- ;Val(V)- ;Ala(A)- ;Gly(G)- ;Leu(L)- ;Ser(S)- ; Asp(D)-

Figure 2: Amino acid composition of *Ap*DXS protein

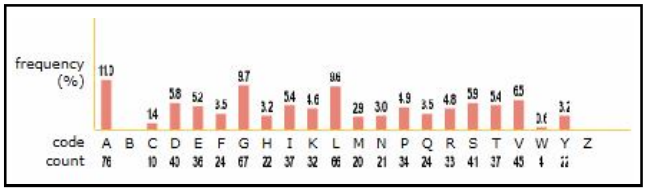

Figure 3: Frequency of amino acids in *Ap*DXS protein

Table 1: Percentage of amino acids in the *Ap*DXS protein sequence

AA:	A	G	L	V	S
% of AA:	11.0	9.7	9.6	6.5	5.9
AA:	D	T	I	E	P
% of AA:	5.8	5.4	5.4	5.2	4.9
AA:	R	K	Q	F	Y
% of AA:	4.8	4.6	3.5	3.5	3.2
AA:	H	N	M	C	W
% of AA:	3.2	3.0	2.9	1.4	0.6

*****result obtained from PHD secondary structure prediction analysis

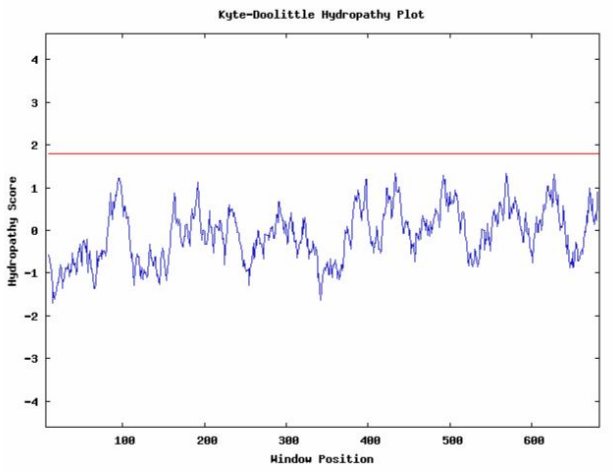

(A)

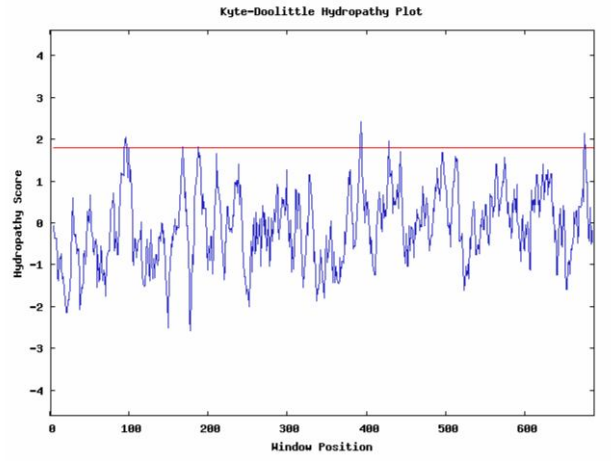

(B)

Figure 8: Hydropathy plot of *Ap*DXS (Picture A: window 19, Picture B: window 9)

The window position values shown on the X-axis of the graph reflect the average hydropathy of the entire window, with the corresponding amino acid as the middle element of that window. Notice that the horizontal axis is scaled to include only those amino acids for which a windowed hydropathy score is computed (Figure 9).

Figure 9: Hydropathy plot of *Ap*DXS

3.2 Characterization of secondary structure, sub-cellular location and signal peptide

Secondary structure predictions revealed the secondary structure of *Ap*DXS consists of 12% turns, 38% helix, 47% coil and 13% extended strands as shown in the pie diagram (Figure 4, 5 and 6). Residues with a scale reliability index of prediction of 5 and over (uppercase letters) are predicted at better than 82%. The percentage of amino acids buried inside the helices is more than 50% whereas 30% amino acids were exposed to outside. Around 10% amino acids of protein were calculated as intermediate by predict protein tool (Figure 7).

Subcellular localization findings by different tools indicated, *Ap*DXS was located in chloroplast. No signal peptide sequence was found in *Ap*DXS though it is encoded by nuclear genome (Perello *et al.*, 2016). Prediction of protein revealed that *Ap*DXS was located in the stroma of chloroplast which is correlated to previous findings in *Arabidopsis* (Hsieh *et al.*, 2008; Zybailov *et al.*, 2008; Joyard *et al.*, 2009; Pulido *et al.*, 2012). *Ap*DXS was predicted as non-secretory protein.

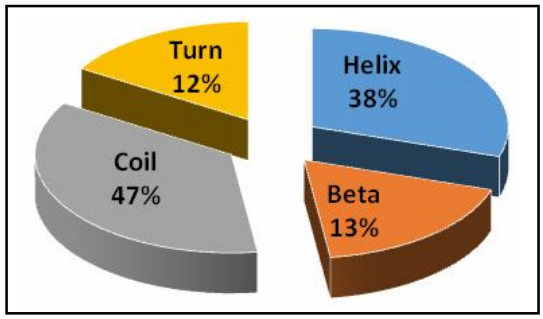

Figure 4: Pie diagram representing the secondary structure composition of *Ap*DXS protein

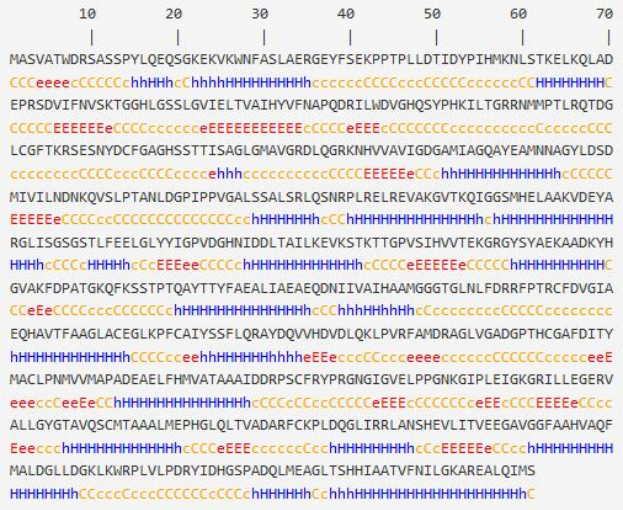

Figure 5: Secondary structure of each amino acids in the *Ap*DXS protein (Hh- Alpha helix; Ee- Extended strand; Cc- Random coil).

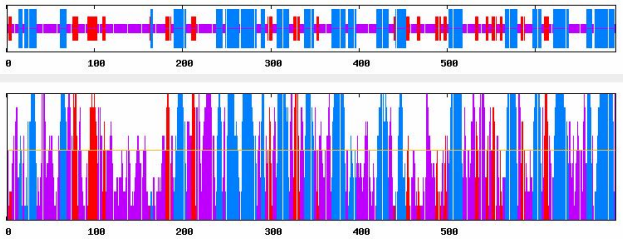

Figure 6: Secondary structure of *Ap*DXS

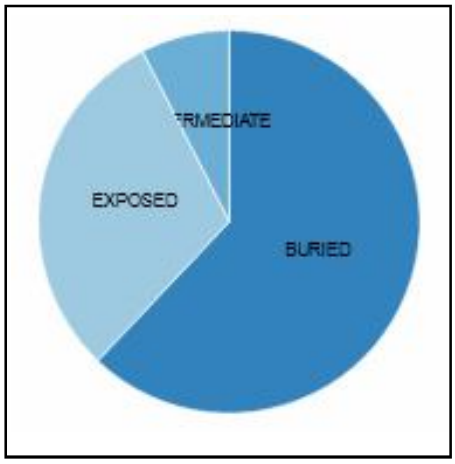

Figure 7: Protein accessibility prediction of *Ap*DXS using PREDICT PROTEIN tool

3.3 Motifs and domain analysis in *Ap*DXS

*Ap*DXS was identified as non-trans membrane protein. *Ap*DXS protein belongs to transketolase super family containing six motifs such as N-terminal DXS synthase motif, C-terminal TPP binding domain, transketolase thiamine diphosphate binding domain, pyruvate-ferredoxin oxidoreductase domain II, transketolase pyrimidine binding domain and transketolase C-terminal domain (Figure 10). Positions of the motifs were represented in the tabular form (Table 2). Pyrimidine binding pocket is a conserved domain found in other organisms could be used as an important basis for determining genetic relationships among species (Shi *et al*, 2016; Goswami, 2017).

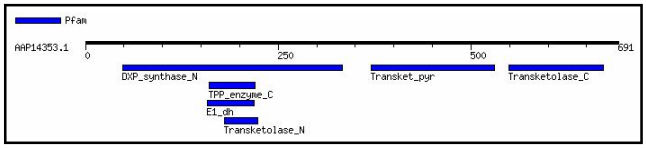

Figure 10: Motif analysis of *Ap*DXS.

Table 2: Different motifs identified in the *Ap*DXS protein and their positions.

Motif	Position	Description
DXS_synthase_N	48-333	1-deoxy D-xylulose 5-phosphate synthase super family
Transket_pyr	371-531	Transketolase, pyrimidine binding domain
Transketolase_C	549-672	Transketolase, C terminal domain
TPP_enzyme_C	161-220	Thiamine pyrophosphate enzyme, C-terminal TPP binding domain
E1_dh	158-219	Dehydrogenase E1 component
Transketolase_N	180-223	Transketolase, thiamine diphosphate binding domain

3.4 3D structural modelling and its validation

3.4.1 3D structural modelling of *Ap*DXS

3D model revealed N terminus of the protein started with Blue ribbons and Red colour bands were C-terminus (Figure 11). Humans and other microorganisms use exclusively MVA pathway for the synthesis of isoprenoids whereas plants relay on MEP pathway. This makes the enzymes of MEP pathway, with particular reference to DXS as attractive drug targets for developing anti-infective and herbicidal models (Masini *et al*., 2015). However, the intermediates of the MEP pathway are phosphorylated which makes designing of drugs is a challenging task (Sanders *et al*., 2017). Finding the ligand binding sites of these enzymes will be helpful in understanding drug-target relationships as reported earlier by Masini *et al*., 2014. The present work in *A. paniculata* brings about first structural insight into the DXS protein and forms the basis for designing future drugs.

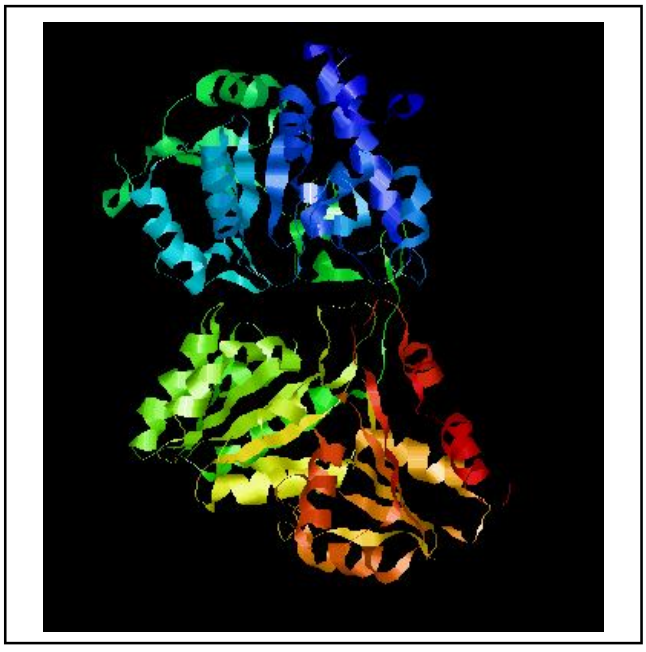

Figure 11: 3D structure of *Ap*DXS

3.4.2 Validation of 3D structure

3D analysis showed 96.32 % of the residues had an averaged 3D-1D score >= 0.2, and indicated the quality of the predicted 3D model of *Ap*DXS was structurally reliable. Amino acids up to 85% were observed in the most favoured regions in Ramachandran plot (Figure 12). Only 1% of amino acids were found in disallowed regions. Overall G-factor was observed as zero which indicated that the structure was not out-of-the-ordinary and not unusual. Only 4 amino acids (Arg 521, 559, Val 115, Leu 228 and Thr 83) were observed in disallowed regions of Ramachandran plot (Figure 12).

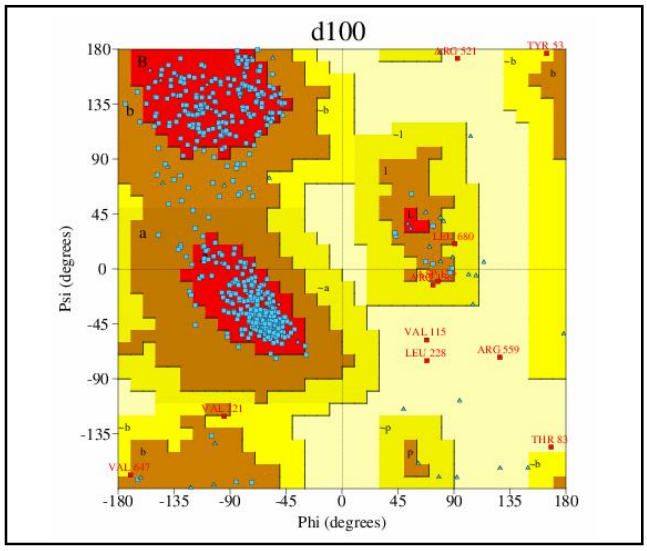

Figure 12: Ramachandran plot of *Ap*DXS 3D structure. The most favored regions are colored red, additional allowed, generously allowed and disallowed regions are indicated as yellow, light yellow and white fields, respectively

3.4.3 Ligand binding

Confidence data from search of structural library was observed with Mammoth 32.9 (Max.-56 and Min.-24.84) when submitted for Ligand binding site prediction (Figure 13). Possible heterogens observed were non-metallic TPP and metallic Mg^{+2} binding sites (Figure 14 and 15). The active site information and super imposed ligands in the ligand binding site was depicted in Figure 16, respectively. This present finding has given more insights on the ligand binding interactions to design drugs in credence with the observations earlier (Saggu *et al*., 2016; Naz *et al*., 2017; Goswami, 2017).

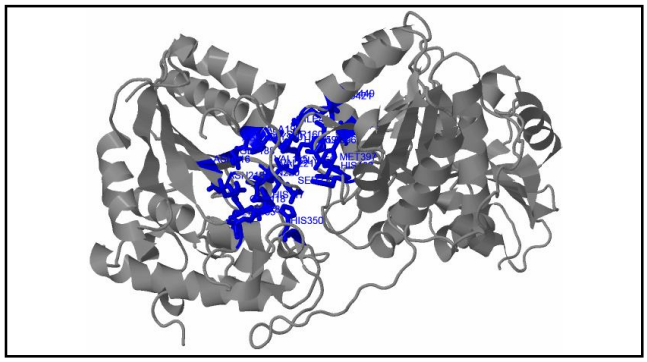

Figure 13: Ligand binding site predicted in *Ap*DXS

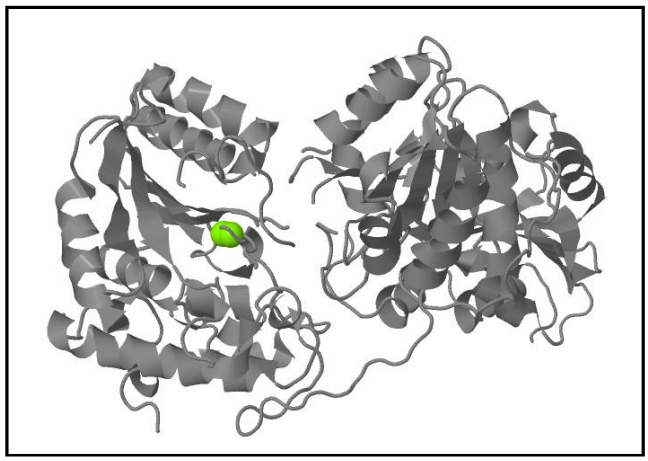

Figure 14: Metallic ligand / Heterogen of *Ap*DXS

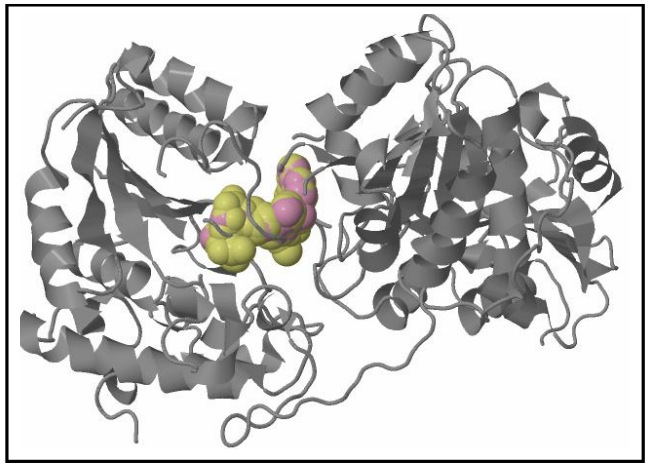

Figure 15: Non-metallic ligand / heterogen of *Ap*DXS

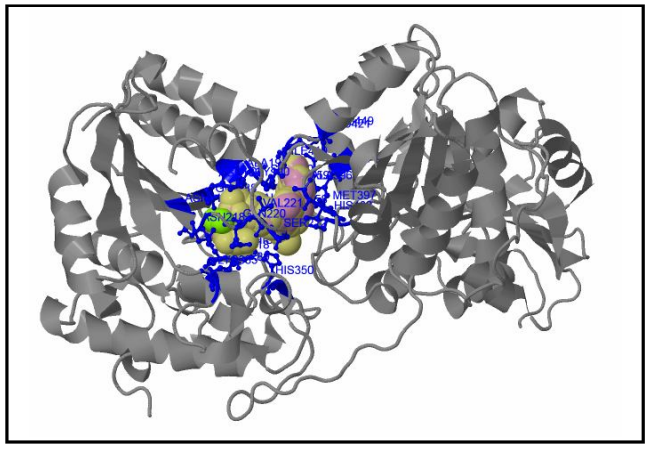

Figure 16: Metallic and non-metallic heterogens bound in the ligand binding pocket of *Ap*DXS

3.5 Evolutionary relationship of *Ap*DXS

*Ap*DXS was shown close relationship with the common ancestor of the plants, *Sesamum indicum* and *Phlomis umbrosa* under same order Lamiales (Figure 17). *Ap*DXS was neighbouring kin with

Lamiaceae and Pedaliaceae. Apart from Lamiaceae and Pedaliaceae was found near to Solanaceae family members, namely; *Withania sominfera, Solanum tuberosum, Solanum lycopersicum, Osmanthus fragrans* and *Capsicum annum* with boot strap value 0.11. The present finding on closely related plants to *A. paniculata* would be beneficial in primer designing, isolation of genes and study associated with regulation of biosynthetic pathways (Jia *et al*., 2016). The evolutionary identity of *Ap*DXS with the related plants will help in isolation of DXS gene in *A. paniculata*. DXS gene have also been cloned and characterized in plants such as *S. lycopersicum, Catharanthus roseus, Ginkgo biloba* and *Aquilaria sinensis* (Chahed *et al*., 2000; Lois *et al*., 2000; Gong *et al*., 2006; Xu *et al*., 2014).

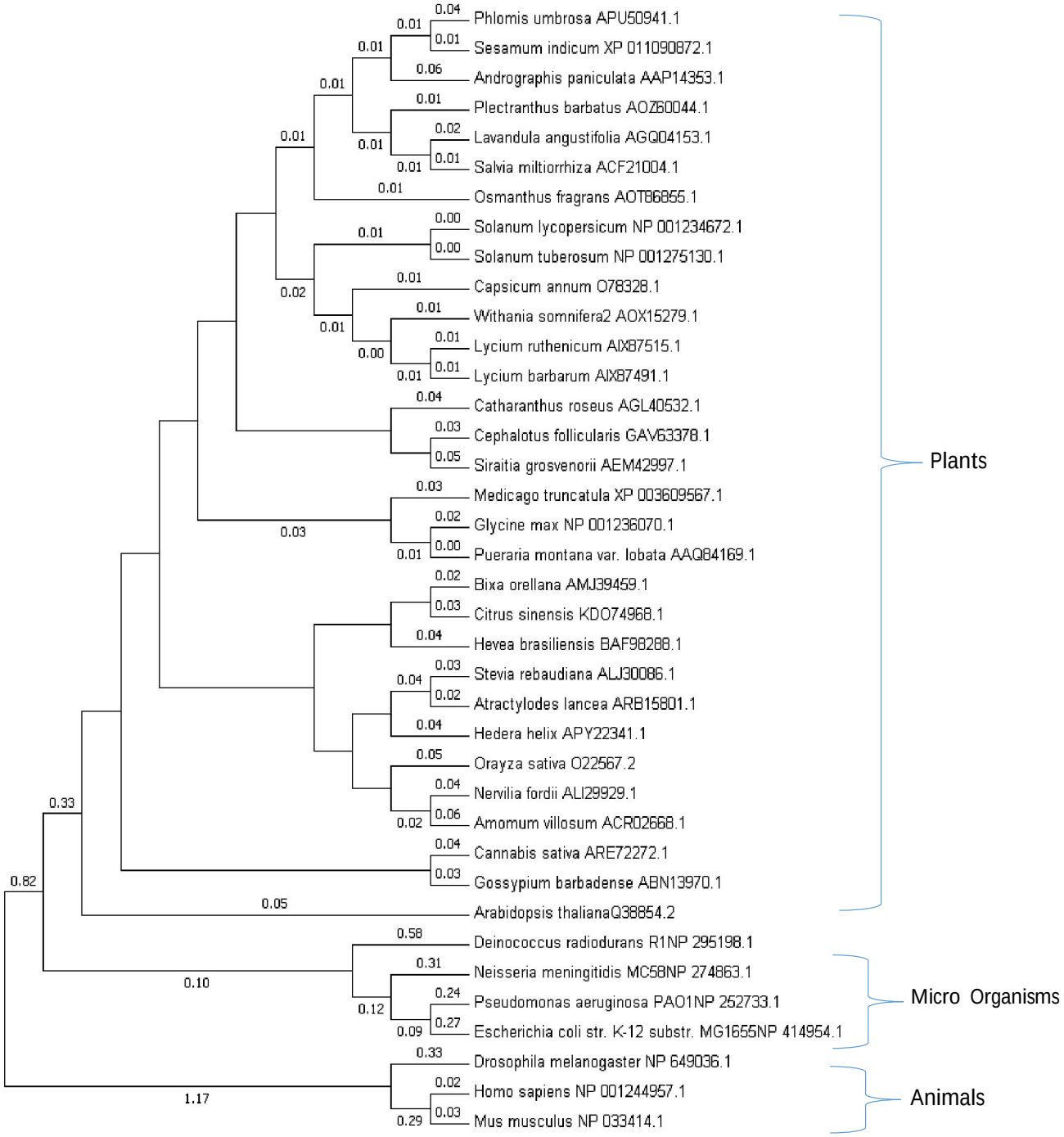

Figure 17: Phylogenetic tree of *Ap*DXS with other DXS proteins amongst the plants, microorganism and other animals.

3.6 Interaction of genes/proteins

*Ap*DXS protein (otherwise called CLA1 protein in *Arabidopsis*) was shown interactions with proteins such as HDR, DXR, HDS, CDPMEK involved in MEP pathway. *Ap*DXS was also observed to interact with MVA pathway protein HMGS and downstream proteins of terpenoid pathway such as IPP1, GPS1 (Figure 18). The finding on protein interactions such as stable physical interactions (direct), functional associating protein interactions, transient binding interactions and information based interactions (indirect) will help in deciphering the function of proteins. The interaction with other pathway proteins (DXS with HMGS) will be an interesting association to study the cross talk between MEP and MVA pathways (Hemmerlin *et al*., 2003; Laule *et al*., 2003; Rodríguez-Concepción *et al*., 2004). The association of *Ap*DXS with downstream proteins will give more insights into the biosynthetic pathway of andrographolide.

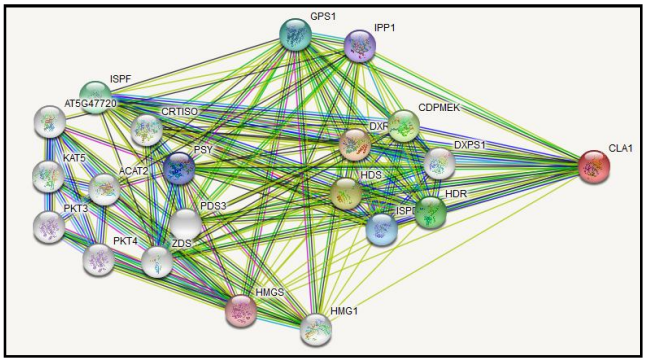

Figure 18: Protein interactions of *Ap*DXS with other pathway related proteins using search tool for the retrieval of interacting genes / protein (STRING) analysis.

In *Arabidopsis* DXS was shown co expression with other MEP proteins such as HDR, CDPMEK, HDS and DXR but not with HMGS, IPP1 and GPS1. Co expression analysis of DXS with other proteins is depicted in the Figure 19. *Oryza sativa* and other organisms such as *E. coli, Mycobacterium tuberculosis, Salmonella enteric, Chlamydomonas reinhardtii, Pseudomonas aeruginosa, Populus trichocarpa, Plasmodium falciparum* DXS protein has shown low level of co expression with IPP1 and ISPD proteins. The co expression studies will be useful for studying the differential expression of proteins and gene regulation in biosynthetic pathway of andrographolide.

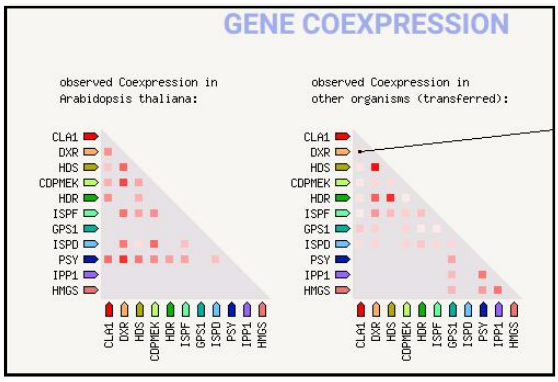

Figure 19: Co expression of DXS protein with other interacting proteins in *Arabidopsis* and other organisms.

4. Conclusion

*Ap*DXS plays a key regulatory role in andrographolide biosynthesis. As there is very less information available about the *Ap*DXS protein, the present *in silico* structural analysis will help in isolation and purification of protein. A reliable 3D model of *Ap*DXS was successfully predicted *in silico*. The predicted 3D model can be used for the drug designing and enzyme inhibition studies in the biosynthetic pathway. The structural information can also be used to study the ligand/regulator binding interactions to alter the role of DXS in the MEP pathway. Evolutionary relations of *Ap*DXS with Lamiaceae family members will be valuable in primer designing for the isolation of DXS gene and study the differential expression of DXS upon elicitation for the enhanced production of andrographolide. Further, interactions study between DXS with HMGS and downstream proteins IPP1, GPS1 will give deep understanding about the exchange of molecules between the two pathways and regulation of metabolic flux.

Acknowledgements

We would like to acknowledge the financial support from OU-UGC-CPEPA programme sponsored by University Grants Commission (UGC), New Delhi. Authors also thank OU-UGC-CPEPA programme and UGC-BSR-RFSMS for research fellowships to MS, AS and BBVB.

Conflict of interest

We declare that we have no conflict of interest.

References

Akbar, S. (2011). *Andrographis paniculata*: A review of pharmacological activities and clinical effects. Altern. Med. Rev., **16**(1):66-77.

Altschul, S.F.; Madden, T.L.; Schäffer, A.A.; Zhang, J.; Zhang, Z.; Miller, W. and Lipman, D.J. (1997). Gapped BLAST and PSI-BLAST: A new generation of protein database search programs. Nucleic Acids Res., **25**(17):3389-3402.

Arolla, R.G.; Cherukupalli, N.; Rao, K.V. and Reddy, V.D. (2015). DNA barcoding and haplotyping in different species of *Andrographis*. Biochem. Syst. Ecol., **62**:91-97.

Bagos, P.G.; Liakopoulos, T.D.; Spyropoulos, I.C. and Hamodrakas, S.J. (2004). PRED-TMBB: A web server for predicting the topology of beta-barrel outer membrane proteins. Nucleic Acids Res., **32**(Web Server issue):W400-4.

Bagos, P.G.; Liakopoulos, T.D.; Spyropoulos, I.C. and Hamodrakas, S.J. (2004). A Hidden Markov model method, capable of predicting and discriminating beta-barrel outer membrane proteins. BMC Bioinformatics, **5**:29-42.

Banerjee, A. and Sharkey, T. D. (2014). Methylerythritol-4-phosphate (MEP) pathway metabolic regulation. Nat. Prod. Rep., **31**(8):1043-1055.

Bannai, H.; Tamada, Y.; Maruyama, O.; Nakai, K. and Miyano, S. (2002). Extensive feature detection of N-terminal protein sorting signals. Bioinformatics, **18**(2):298-305.

Bannai, H.; Tamada, Y.; Maruyama, O.; Nakai, K. and Miyano, S. (2001). Views: Fundamental building blocks in the process of knowledge discovery. In: Proceedings of the 14th International FLAIRS Conference., 233-238.

Bindu, B.B.V.; Srinath, M.; Shailaja, A. and Giri, C.C. (2017). Comparative protein profile studies and *in silico* structural / functional analysis of HMGR (ApHMGR) in *Andrographis paniculata* (Burm. f.) Wall. ex Nees. Ann. Phytomed., **6**(1):30-44.

Bjellqvist, B.; Hughes, G.J.; Pasquali, Ch.; Paquet, N.; Ravier, F.; Sanchez, J.Ch.; Frutiger, S. and Hochstrasser, D.F. (1993). The focusing positions of polypeptides in immobilized pH gradients can be predicted from their amino acid sequences. Electrophoresis, **14**:1023-1031.

Bjellqvist, B.; Basse, B.; Olsen, E. and Celis, J.E. (1994). Reference points for comparisons of two-dimensional maps of proteins from different human cell types defined in a pH scale where isoelectric points correlate with polypeptidecompositions. Electrophoresis, **15**:529-539.

Chahed, K.; Oudin, A.; Guivarc'h, N.; Hamdi, S.; Chénieux, J.C.; Rideau, R.; Clastre, M. (2000). 1-Deoxy-d-xylulose 5-phosphate synthase from periwinkle: cDNA identification and induced gene expression in terpenoid indole alkaloid- producing cells, Plant Physiology and Biochemistry, **38**:559-566.

Cordoba, E.; Salmi, M.; León, P. (2009). Unravelling the regulatory mechanisms that modulate the MEP pathway in higher plants, J. Exp. Bot., **60**:2933-2943.

Cordoba, E.; Porta, H.; Arroyo, A.; San Román, C.; Medina, L.; Rodríguez-Concepción, M. and León, P. (2011). Manuel Rodríguez-Concepción, Patricia León; functional characterization of the three genes encoding 1-deoxy-D-xylulose 5- phosphate synthase in maize. J. Exp. Bot., **62**(6):2023-2038.

Cserzo, M.; E. Wallin, I.; Simon, G.; Heijne, V. and Elofsson, A. (1997). Prediction of trans-membrane alpha-helices in prokaryotic membrane proteins: The Dense Alignment Surface method. Protein. Eng., **10**:(6):673-676.

Cuff, J. A.; Clamp, M. E.; Siddiqui, A. S.; Finlay, M. and Barton, G. J. (1998). Jpred: A Consensus Secondary Structure Prediction Server. Bioinformatics, **14**:892-893,

Ebina, T.; Toh, H. and Kuroda, Y. (2009). Loop length dependent SVM prediction of domain linkers for high throughput structural proteomics. Biopolymers, **92**(1):1-8.

Eisenberg, D.; Weiss, R.M.; Terwilliger, T.C. (1982). The helical hydrophobic moment: A measure of the amphiphilicity of a helix. Nature, **299**(5881):371-4.

Eisenreich, W.; Bacher, A.; Arigoni, D. and Rohdich, F. (2004). Biosynthesis of isoprenoids *via* the non-mevalonate pathway. Cell Mol. Life Sci., **61**:1401-1426.

Emanuelsson, O.; Brunak, S.; Von Heijne, G. and Nielsen, H. (2007). Locating proteins in the cell using TargetP, SignalP and related tools. Nat. Protoc., **2**(4):953-971.

Emanuelsson, O.; Nielsen, H.; Brunak, S. and Von Heijne, G. (2000). Predicting subcellular localization of proteins based on their N-terminal amino acid sequence. J. Mol. Biol., **300**(4):1005-1016.

Enfissi, E.M.; Fraser, P.D.; Lois, L.M.; Boronat, A.; Schuch, W. and Bramley, P.M. (2005). Metabolic engineering of the mevalonate and nonmevalonate isopentenyl diphosphate-forming pathways for the production of health-promoting isoprenoids in tomato. Plant Biotechnol. J., **3**;17-27.

Estévez, J.M.; Cantero, A.; Reindl, A.; Reichler, S. and León, P. (2001). 1-Deoxy-D-xylulose-5-phosphate synthase, a limiting enzyme for plastidic isoprenoidbiosynthesis in plants. J. Biol. Chem., **276**:22901-22909.

Finn, R.D.; Coggill, P.; Eberhardt, R.Y.; Eddy, S.R.; Mistry, J.; Mitchell, A.L.; Potter, S.C.; Punta, M.; Qureshi, M.; Sangrador-Vegas, A. and Salazar, G.A.; Tate, J. and Bateman, A. (2016). The Pfam protein families database: towards a more sustainable future. Nucleic Acids Res., **44**(D1): D279-D285.

Finn, R.D. Attwood, T.K.; Babbitt, P.C.; Bateman, A.; Bork, P.; Bridge, A.; Chang, H.Y.; Dosztányi, Z.; El-Gebali, S.; Fraser, M.; Gough, J.; Haft, D.; Holliday, G.L.; Huang, H.; Huang, X.; Letunic, I.; Lopez, R.; Lu, S.; Marchler-Bauer, A.; Mi, H.; Mistry, J.; Natale, D.A.; Necci, M.; Nuka, G.; Orengo, C.A.; Park, Y.; Pesseat, S.; Piovesan, D.; Potter, S.C.; Rawlings, N.D.; Redaschi, N.; Richardson, L.; Rivoire, C.; Sangrador-Vegas, A.; Sigrist, C.; Sillitoe, I.; Smithers, B.; Squizzato, S.; Sutton, G.; Thanki, N.; Thomas, P.D.; Tosatto, S.C.; Wu, C.H.; Xenarios, I.; Yeh, L.S.; Young, S.Y. and Mitchell, A.L. (2016). InterPro in 2017-beyond protein family and domain annotations. Nucleic Acids Res., **45**(D1):D190-D199.

Frank, A. and Groll, M. (2016). The methylerythritol phosphate pathway to isoprenoids. Chemical Rev., **117**(8):5675-703.

García-Alcázar, M.; Giménez, E.; Pineda, B.; Capel, C.; García-Sogo, B.; Sánchez, S.; Yuste-Lisbona, F.J.; Angosto, T.; Capel, J.; Moreno, V. and Lozano, R. (2017). Albino T-DNA tomato mutant reveals a key function of 1-deoxy-D-xylulose-5- phosphate synthase (DXS1) in plant development and survival. Sci. Rep., **7**:1-12.

Gasteiger, E.; Hoogland, C.; Gattiker, A.; Duvaud, S.; Wilkins, M.R.; Appel, R.D. and Bairoch, A, (2005). Protein identification and analysis tools on the ExPASy server. In: John M. Walker (ed): The Proteomics Protocols Handbook, Humana Press, 571-607.

Gong, Y.F.; Liao, Z.H.; Guo, B.H.; Sun, X.F. and Tang, K.X. (2006). Molecular cloning and expression profile analysis of *Ginkgo biloba* DXS gene encoding 1-deoxy-d- xylulose 5-phosphate synthase, the first committed enzyme of the 2-C-methyl-d-erythritol 4-phosphate pathway. Planta Med., **72**:329-335

Goswami, A. M. (2017). Computational analysis, structural modeling and ligand binding site prediction of *Plasmodium falciparum* 1-deoxy-d-xylulose-5-phosphate synthase. Comput. Biol. Chem., **66**:1-10.

Guevara-García, A.A.; San Roman, C.; Arroyo, A.; Cortés, M.E.; Gutiérrez-Nava, M.L. and León, P. (2005). The characterization of the *Arabidopsis* clb6 mutant illustrates the importance of post-transcriptional regulation of the methyl-D-erythritol 4-phosphate pathway. Plant Cell, **17**:628-643.

Harker, M. and Bramley, P.M. (1999). Expression of prokaryotic-1-deoxy-D-xylulose-5-phosphatases in *Escherichia coli* increases carotenoid and ubiquinone biosynthesis. FEBS Lett., **448**:115-119.

Hemmerlin, A.; Hoeffler, J.F.; Meyer, O.; Tritsch, D. and Isabelle, A. (2003). Cross-talkbetween the cytosolic mevalonate and the plastidial methylerythritol phosphate pathways in tobacco bright yellow-2 cells. J. Biol. Chem., **278**:26666-26676.

Henriquez, M.A.; Soliman, A.; Li, G.; Hannoufa, A.; Ayele, B.T. and Daayf, F. (2016). Molecular cloning, functional characterization and expression of potato (*Solanum tuberosum*) 1-deoxy-d-xylulose 5-phosphate synthase 1 (StDXS1) in response to *Phytophthora infestans*. Plant Sci., **243**:71-83.

Hiller, K.; Grote, A.; Maneck, M.; Münch, R. and Jahn, D. (2006). JVirGel 2.0: computational prediction of proteomes separated via two-dimensional gel electrophoresis under consideration of membrane and secreted proteins. Bioinformatics, **22**:2441-2443.

Hiller, K.; Schobert, M.; Hundertmark, C.; Jahn, D. and Münch, R. (2003). JVirGel: calculation of virtual two-dimensional protein gels. Nucleic Acids Res., **31**:3862-3865.

Hiller, K.; Grote, A.; Scheer, M.; Münch, R. and Jahn, D. (2004). PrediSi: prediction of signal peptides and their cleavage positions. Nucleic Acids Res., **32** (Web Server issue):W375-9.

Hossain, M.S.; Urbi, Z.; Sule, A. and Hafizur Rahman, K.M. (2014). *Andrographis paniculata* (Burm. f.) Wall. ex Nees: A review of ethnobotany, phytochemistry, and pharmacology. Sci. World J. **2014**:1-28.

Hsieh, M.H.; Chang, C.Y.; Hsu, S.J. and Chen, J.J. (2008). Chloroplast localization of methylerythritol 4-phosphate pathway enzymes and regulation of mitochondrial genes in ispD and ispE albino mutants in *Arabidopsis*. Plant Mol. Biol., **66**:663-673.

Hu, X.Y.; Wu, R.H.; Logue, M.; Blondel, C.; Lai, L.Y.W.; Stuart, B.; Flower, A.; Fei, Y.T.; Moore, M.; Shepherd, J.; Liu, J.P. and Lewith, G. (2017). *Andrographis paniculata* (Chuân Xîn Lián) for symptomatic relief of acute respiratory tract infections in adults and children: A systematic review and meta-analysis. PloS. One, **12**(8):0181780.

Jadaun, J. S.; Sangwan, N. S.; Narnoliya, L. K.; Singh, N.; Bansal, S.; Mishra, B. and Sangwan, R. S. (2017). Over expression of DXS gene enhances terpenoidal secondary metabolite accumulation in rose scented geranium and *Withania somnifera:* active involvement of plastid isoprenogenic pathway in their biosynthesis. Physiol. Plant, **159**(4):381-400.

Jia, Q. (2016). Computational Identification of Terpene Synthase Genes and Their Evolutionary Analysis. Ph.D. Thesis., University of Tennessee.

Joyard, J.; Ferro, M.; Masselon, C.; Seigneurin-Berny, D.; Salvi, D.; Garin, J. and Rolland, N. (2009). Chloroplast proteomics and the compartmentation of plastidial isoprenoid biosynthetic pathways. Mol. Plant, **2**(6);1154-1180.

Kelley, L. A.; Mezulis, S.; Yates, C. M.; Wass, M. N. and Sternberg, M. J. (2015). The Phyre2 web portal for protein modeling, prediction and analysis. Nat. Protoc., **10**(6):845-858.

Kim, BR.; Kim, S.U. and Chang, Y.J. (2005). Differential expression of three 1-deoxy-D-xylulose-5-phosphate synthase genes in rice. Biotechnol. Lett., **27**:997-1001.

Krogh, A.; Larsson, B.; Von Heijne, G. and Sonnhammer, E. L. (2001). Predicting trans-membrane protein topology with a hidden Markov model: application to complete genomes. J. Mol. Biol., **305**(3):567-580.

Krushkal, J.; Pistilli, M.; Ferrell, K.M.; Souret, F.F. and Weathers, P.J. (2003). Computational analysis of the evolution of the structure and function of 1-deoxy-D- xylulose-5-phosphate synthase, a key regulator of the mevalonate-independent pathway in plants. Gene, **313**:127-138.

Kudoh, K.; Hotta, S.; Sekine, M.; Fujii, R.; Uchida, A.; Kubota, G.; Kawano, Y. and Ihara, M. (2017). Overexpression of endogenous 1-deoxy-d-xylulose 5-phosphate synthase (DXS) in cyanobacterium *Synechocystis sp*. PCC6803 accelerates protein aggregation. J. Biosci. Bioeng., **123**(5):590-596.

Kumar, S.; Stecher, G. and Tamura, K. (2016). MEGA7: Molecular Evolutionary Genetics Analysis version 7.0 for bigger datasets. Mol. Biol. Evol., **33**(7):1870-1874.

Kuzuyama, T.; Takagi, M.; Takahashi, S and Seto, H. (2000). Cloning and characterization of 1-deoxy-D-xylulose 5-phosphate synthase from *Streptomyces sp*. strain CL190, which uses both the mevalonate and nonmevalonate pathways for isopentenyl diphosphate biosynthesis. J. Bacteriol., **182**;891-897.

Kyte, J. and Doolittle, R.F. (1982). A simple method for displaying the hydropathic character of a protein. J. Mol. Biol., **157**(1):105-132.

Lange, B.M.; Wildung, M.R.; McCaskill, D. and Croteau, R. (1998). A family of transketolases that directs isoprenoid biosynthesis via a mevalonate-independent pathway. Proc. Natl. Acad. Sci. USA., **95**:2100-2104.

Laskowski, R.A.; MacArthur, M.W.; Moss, D. S. and Thornton, J.M. (1993). PROCHECK- A program to check the stereochemical quality of protein structures. J. App. Cryst., **26**:83-291.

Laule, O.; Furholz, A.; Chang, H.S.; Zhu, T. and Wang, X. (2003). Crosstalk between cytosolic and plastidial pathways of isoprenoid biosynthesis in *Arabidopsis thaliana*. Proc. Natl. Acad. Sci. USA **100**:6866-6871.

Lois, L.M.; Rodriguez-Concepcion, M.; Gallego, F.; Campos, N. and Boronat, A. (2000). Carotenoid biosynthesis during tomato fruit development, regulatory role of 1-deoxy- d-xylulose 5-phosphate synthase. Plant. J., **22**:503-513.

Lois, L.M.; Campos, N.; Rosa-Putra, S.; Danielsen, K.; Rohmer, M. and Boronat, A. (1998). Cloning and characterization of a gene from *Escherichia coli* encoding a transketolase-like enzyme that catalyzes the synthesis of D-1-deoxyxylulose 5-phosphate, a common precursor for isoprenoid, thiamin, and pyridoxol biosynthesis, Proc. Natl. Acad. Sci. USA., **95**:2105-2110.

Masini, T.; Lacy, B.; Monjas, L.; Hawksley, D.; De Voogd, A.R.; Illarionov, B.; Iqbal, A.; Leeper, F.J.; Fischer, M.; Kontoyianni, M. and Hirsch, A.K.H. (2015). Validation of a homology model of *Mycobacterium tuberculosis* DXS: rationalization of observed activities of thiamine derivatives as potent inhibitors of two orthologues of DXS. Org. Biomol. Chem., **13**(46):11263-11277.

Masini, T. and Hirsch, A. K. (2014). Development of Inhibitors of the 2 C-Methyl-d-erythritol 4-Phosphate (MEP) Pathway Enzymes as Potential Anti-Infective Agents. J. Med. Chem., **57**(23):9740-9763.

Mendoza-Poudereux, I.; Kutzner, E.; Huber, C.; Segura, J.; Eisenreich, W. and Arrillaga, I. (2015). Metabolic cross-talk between pathways of terpenoid backbone biosynthesis in spike lavender. Plant. Physiol. Biochem., **95**:113-120.

Morris, W.L.; Ducreux, L.J.; Hedden, P.; Millam, S. and Taylor, M.A. (2006). Overexpression of a bacterial 1-deoxy-D-xylulose 5-phosphate synthase gene in potato tubers perturbs the isoprenoid metabolic network: implications for the control of the tuber life cycle. J. Exp. Bot., **57**:3007-3018.

Naz, S.; Ngo, T.; Farooq, U. and Abagyan, R. (2017). Analysis of drug binding pockets and repurposing opportunities for twelve essential enzymes of ESKAPE pathogens. Peer J., **5**:e3765.

Neeraja, C.; Krishna, P.H.; Reddy, C.S.; Giri, C.C.; Rao, K.V. and Reddy, V.D. (2015). Distribution of *Andrographis* species in different districts of Andhra Pradesh. Proc. Natl. Acad. Sci. India Sect. B. Biol. Sci., **85**:601-606.

Neeraja, C.; Mayur, D.; Mittapelli, S.R.; Rao, K.V. and Reddy, V.D. (2016). Denovo assembly of leaf transcriptome in the medicinal plant **Andrographis paniculata**. Front. Plant Sci., **7**:1-13

Nielsen, H.; Engelbrecht, J.; Brunak, S. and Von Heijne, G. (1997). Identification of prokaryotic and eukaryotic signal peptides and prediction of their cleavage sites. Protein Eng., **10**:1-6.

Nyeem, M. A.; Mannan, M. A.; Nuruzzaman, M.; Kamrujjaman, K. M. and Das, S. K. (2017). Indigenous king of bitter (*Andrographis paniculata*): A review. J. Med. Plant Stud., **5**(2); 318-324.

Okhuarobo, A.; Falodun, J.E.; Erharuyi, O.; Imieje, V.; Falodun, A. and Langer, P. (2014). Harnessing the medicinal properties of *Andrographis paniculata* for diseases and beyond: a review of its phytochemistry and pharmacology. Asian Pac. J. Trop. Dis., **4**(3):213-222.

Parlapally, S.; Cherukupalli, N.; Bhumireddy, S.R.; Sripadi, P.; Anisetti, R.; Giri, C.C. and Reddy, V.D. (2 015). Chemical profiling and anti-psoriatic activity of methanolic extract of *Andrographis nallamalayana* J.L. Ellies. Nat. Prod. Res., 30:1256-1261.

Perello, C.; Llamas, E.; Burlat, V.; Ortiz-Alcaide, M.; Phillips, M. A.; Pulido, P. and Rodriguez-Concepcion, M. (2016). Differential subplastidial localization andturnover of enzymes involved in isoprenoid biosynthesis in chloroplasts. PloS One, **11**(2):e0150539.

Petersen, T.N.; Brunak, S.; von Heijne, G. and Nielsen, H. (2011). SignalP 4.0: discriminating signal peptides from trans-membrane regions. Nat. Methods., **8**(10):785-786.

Phillips, M.A.; León, P.; Boronat, A. and Rodríguez-Concepción, M. (2008). The plastidial MEP pathway: unified nomenclature and resources. Trends. Plant. Sci., **13**:619-623.

Pulido, P.; Perello, C. and Rodriguez-Concepcion, M. (2012). New insights into plant isoprenoid metabolism. Mol. Plant., **5**(5):964-967.

Rodríguez-Concepción, M. and Boronat, A. (2015). Breaking new ground in the regulation of the early steps of plant isoprenoid biosynthesis. Curr. Opin. Plant Biol., **25**:17-22.

Rodríguez-Concepción, M.; Fores, O.; Martinez-Garcia, J.F.; Gonzalez, V. and Phillips, M.A. (2004). Distinct light-mediated pathways regulate the biosynthesis and exchange of isoprenoid precursors during Arabidopsis seedling development. Plant Cell, **16**:144-56.

Rodríguez-Concepción, M. (2004). The MEP pathway: a new target for the development of herbicides, antibiotics and antimalarial drugs. Curr. Pharm. Des., **10**:2391-2400.

Rodríguez-Villalón, A.; Gas, E. and Rodríguez-Concepción, M. (2009). Phytoene synthase activity controls the biosynthesis of carotenoids and the supply of their metabolic precursors in dark-grown *Arabidopsis* seedlings. Plant. J., **60**:424-435.

Rohmer, M.; Seemann, M.; Horbach, S.; Bringer-Meyer, S. and Sahm, H. (1996). Glyceraldehyde 3-phosphate and pyruvate as precursors of isoprenic units in an alternative non-mevalonate pathway for terpenoid biosynthesis. J. Am. Chem. Soc., **118**:2564-2566.

Rost, B.; Yachdav, G. and Liu, J. (2004). The PredictProtein server. Nucleic. Acids. Res., **32**(Web Server issue):W321-6.

Saggu, G.S.; Pala, Z.R.; Garg, S. and Saxena, V. (2016). New insight into isoprenoids biosynthesis process and future prospects for drug designing in Plasmodium. Front. Microbiol., **7**:1421.

Sanchita; Singh, S. and Sharma, A. (2014). Bioinformatics approaches for structural and functional analysis of proteins in secondary metabolism in *Withania somnifera*. Mol. Biol. Rep., **41**(11):7323-7330.

Sanders, S.; Vierling, R.J.; Bartee, D.; DeColli, A.A.; Harrison, M.J.; Aklinski, J.L.; Koppisch, A.T. and Freel Meyers, C.L. (2017). Challenges and hallmarks of establishing alkylacetylphosphonates as probes of bacterial 1-deoxy-d-xylulose 5-phosphate synthase. ACS Infect. Dis., **3**(7):467-478.

Sharma, P. and Sanadhya, D. (2017). The King of Bitters," *Andrographis paniculata*": A Plant with Multiple Medicinal Properties. J. Plant Sci. Res., **33**(1):117.

Shi, P.; Cao, H.; Li, D.; Wang, Y. and Lei, X. (2016). Bioinformatics analysis of DXS gene from six tropical plants including oil palm (*Elaeis guineensis Jacq*.). Guangxi Zhiwu/Guihaia, **36**(4):471-478.

Simpson, K.; Quiroz, L.F.; Rodriguez-Concepción, M. and Stange, C. R. (2016). Differential contribution of the first two enzymes of the MEP pathway to the supply of metabolic precursors for carotenoid and chlorophyll biosynthesis in carrot (*Daucus carota*). Front. Plant. Sci., **7**:1344.

Srivastava, N. and Akhila, A. (2010). Biosynthesis of andrographolide in *Andrographis paniculata*. Phytochemistry, **71**(11):1298-1304.

Subramanian, R.; Asmawi, M.Z. and Sadikun, A. (2012). A bitter plant with a sweet future? A comprehensive review of an oriental medicinal plant: *Andrographis paniculata*. Phytochem.Rev., **11**(1):39-75.

Sweet, R.M. and Eisenberg, D. (1983). Correlation of sequence hydrophobicities measures similarity in three-dimensional protein structure. J. Mol. Biol., **171**(4):479-488.

Szklarczyk, D.; Franceschini, A.; Wyder, S.; Forslund, K.; Heller, D.; Huerta-Cepas, J.; Simonovic, M.; Roth, A.; Santos, A.; Tsafou, K.P.; Kuhn, M.; Bork, P.; Jensen, L.J. and Von Mering, C. (2014). STRING v10: protein-protein interaction networks, integrated over the tree of life. Nucleic Acids Res., **43**(D1):D447-D452.

Tusnády, G.E. and Simon, I. (1998). Principles Governing Amino Acid Composition of Integral Membrane Proteins: Applications to Topology Prediction. J. Mol. Biol., **283**:489-506.

Tusnády, G.E. and Simon, I. (2001). The HMMTOP trans-membrane topology predictionserver. Bioinformatics, **17**:849-850.

Walter, M.; Hans, J. and Strack, D. (2002). Two distantly-related genes encoding 1-deoxy-D-xylulose 5-phosphate synthases: Differential regulation in shoots andapocarotenoid-accumulating mycorrhizal roots. Plant. J., **31**:243-254.

Wass, M.N.; Kelley, L.A. and Sternberg, M.J. (2010). 3DLigandSite: predicting ligand- binding sites using similar structures. Nucleic. Acids. Res., **38**:W469-73.

Wright, L.P.; Rohwer, J.M.; Ghirardo, A.; Hammerbacher, A.; Ortiz-Alcaide, M.; Raguschke, B.; Schnitzler, J.P.; Gershenzon, J. and Phillips, M.A. (2014). Deoxyxylulose 5-phosphate synthase controls flux through the methylerythritol 4-phosphate pathway in *Arabidopsis*. Plant Physiol., **165**(4):1488-1504.

Xu, Y.H.; Liu, J.; Liang, L.; Yang, X.; Zhang, Z.; Gao, Z.H.; Sui, C. and Wei, J.H. (2014). Molecular cloning and characterization of three cDNAs encoding 1-deoxy-d- xylulose-5-phosphate synthase in *Aquilaria sinensis* (Lour.) Gilg. Plant Physiol. Biochem., **82**:133-141

Yang, J.; Adhikari, M.N.; Liu, H.; Xu, H.; He, G.; Zhan, R.; Wei, J. and Chen, W. (2012). Characterization and functional analysis of the genes encoding 1-deoxy-D-xylulose-5-phosphate reductoisomerase and 1-deoxy-D-xylulose-5-phosphate synthase, the two enzymes in the MEP pathway, from *Amomum villosum* Lour. Mol. Biol. Rep., **39**(8):8287-8296.

Yaqoob, U.; Kaul, T. and Nawchoo, I.A. (2016). *In silico* analysis, structural modelling and phylogenetic analysis of acetohydroxyacid synthase gene of *Oryza sativa*. Med. Aromat. Plants (Los Angel), **5**(272) : 2167-0412.

Yu, C.S.; Lin, C.J. and Hwang, J.K. (2004). Predicting subcellular localization of proteins for Gram-negative bacteria by support vector machines based on n-peptide compositions. Protein Sci., **13**:1402-1406.

Yu, C.S.; Chen, Y.C.; Lu, C.H. and Hwang, J.K. (2006). Prediction of protein subcellularlocalization. Proteins, **64**(3):643-651.

Zaheer, M. and Giri, C.C. (2015). Multiple shoot induction and jasmonic versus salicylic acid driven elicitation for enhanced andrographolide production in *Andrographis paniculata*. Plant Cell Tiss. Organ Cult., **12**(2):553-563.

Zaheer, M. and Giri, C.C. (2017a). Enhanced diterpene lactone (andrographolide) production from elicited adventitious root cultures of *Andrographis paniculata*. Res. Chem. Intermed., **43**:2433-2444.

Zaheer, M. and Giri, C.C. (2017b). Influence of cotyledon, hypocotyl extracts and authentic andrographolide on selective Agrobacterium rhizogenes strains growth: A deterrent to hairy root induction in Andrographis paniculata (Burm.f.) Wall. ex Nees. Ann. Phytomed., **6**(1):51-56.

Zhao, L.; Chang, W.C.; Xiao, Y.; Liu, H.W. and Liu, P. (2013). Methylerythritol phosphate pathway of isoprenoid biosynthesis. Ann. Rev. Biochem., **82**:497-530.

Zhou, W.; Huang, F.; Li, S.; Wang, Y.; Zhou, C.; Shi, M.; Wang, J.; Chen, Y.; Wang, Y.; Wang, H. and Kai, G. (2016). Molecular cloning and characterization of two 1- deoxy-d-xylulose-5-phosphate synthase genes involved in tanshinone biosynthesis in *Salvia miltiorrhiza*. Molecular breeding, **36**(9):124.

Zybailov, B.; Rutschow, H.; Friso, G.; Rudella, A.; Emanuelsson, O.; Sun, Q. and van Wijk, K.J. (2008). Sorting signals, N-terminal modifications and abundance of the chloroplast proteome. PloS One, **3**(4):1994.